



Structural and thermal gas desorption properties of metal aluminum amides

Taisuke Ono^a, Keiji Shimoda^b, Masami Tsubota^b, Satoshi Hino^b,
Ken-ichi Kojima^c, Takayuki Ichikawa^{a,b,*}, Yoshitsugu Kojima^{a,b}

^a Department of Quantum Matter, AdSM, Hiroshima University, Higashi-Hiroshima 739-8530, Japan

^b Institute for Advanced Materials Research, Hiroshima University, Higashi-Hiroshima 739-8530, Japan

^c Division of Environmental Sciences, Graduate School of Integrated Arts and Sciences, Hiroshima University, Higashi-Hiroshima 739-8521, Japan

ARTICLE INFO

Article history:

Received 1 May 2010

Received in revised form 23 June 2010

Accepted 1 July 2010

Available online 8 July 2010

Keywords:

Hydrogen storage

Ammonia

Metal aluminum amide

Mechanical milling

ABSTRACT

Metal aluminum amides $M[\text{Al}(\text{NH}_2)_4]_x$ ($M = \text{K}, \text{Mg}, \text{and Ca}; x = 1 \text{ and } 2$) were synthesized along with previously reported $\text{LiAl}(\text{NH}_2)_4$ and $\text{NaAl}(\text{NH}_2)_4$ by ball milling technique under liquid NH_3 . The profiles of synchrotron radiation X-ray diffraction suggest that $\text{KAl}(\text{NH}_2)_4$, $\text{Mg}[\text{Al}(\text{NH}_2)_4]_2$ and $\text{Ca}[\text{Al}(\text{NH}_2)_4]_2$ have been indexed with single phases, which have never been reported so far. Combination of both FT-IR and ^{27}Al MAS/3QMAS nuclear magnetic resonance suggest that they all have an anion complex unit $[\text{Al}(\text{NH}_2)_4]^-$ as a basic component, indicating successful synthesis of the metal aluminum amides. Thermogravimetry-differential thermal analysis coupled with mass spectroscopy showed the release of NH_3 below the temperatures of 140°C during the thermal decomposition and a NH_3 desorption peak temperature (T_{des}) decreased with the increasing atomic number. Additionally, a relationship between ^{27}Al isotropic chemical shift and T_{des} was discussed. The present study gives an useful information that the thermal stability of the anion complex $[\text{Al}(\text{NH}_2)_4]^-$ can be controlled by a cation M .

© 2010 Elsevier B.V. All rights reserved.

1. Introduction

Global warming and the resource exhaustion are serious problems to be solved. A solution for these problems has been extensively studied. Especially, the construction of a clean energy-oriented society based on hydrogen and the electric power has been paid much attention. To achieve the hydrogen energy society, the development of a hydrogen storage system that has high volumetric and gravimetric hydrogen capacity, high durability, and moderate operating temperature is required. In these days, much interest has been focused on the hydrogen storage materials composed of light elements, so-called chemical hydride [1].

For chemical hydride, a technique to make a composite is quite useful to improve gas desorption properties. This improvement is coming from the fact that the composite takes different reaction pathways from each constituent on heating. In fact, Chen et al. reported that the composite of LiH and LiNH_2 reversibly released 6.3 mass% H_2 at around 200°C [2], although LiH and LiNH_2 themselves decomposed into Li and H_2 above 650°C , and into Li_2NH and NH_3 at 300°C , respectively [3,4]. These facts indicate that making a composite could improve the thermodynamics in the LiH – LiNH_2

system, which can be understood by the NH_3 -mediated reaction mechanism [4]. Recently, Janot et al. focused on $\text{LiAl}(\text{NH}_2)_4$ which is more labile than LiNH_2 and reported that the composite of LiH and $\text{LiAl}(\text{NH}_2)_4$ released more than 5 mass% H_2 below 130°C [5].

Apart from the composite technique, the metal aluminum amides $M[\text{Al}(\text{NH}_2)_4]_x$ themselves are attractive because they indirectly store hydrogen in the form of amide $[\text{NH}_2]^-$. Actually, $\text{LiAl}(\text{NH}_2)_4$ releases 35 mass% of the NH_3 gas with a peak temperature of about 140°C [5–7]. Moreover, Aliouane et al. showed that $\text{NaAl}(\text{NH}_2)_4$ had 30 mass% NH_3 density and the NH_3 desorption peak temperature was about 100°C [8] which was much lower than that of $\text{LiAl}(\text{NH}_2)_4$ [9,10].

In this study, we successfully prepared the metal aluminum amides $M[\text{Al}(\text{NH}_2)_4]_x$ ($M = \text{K}, \text{Mg}, \text{and Ca}; x = 1 \text{ and } 2$), along with previously reported $\text{LiAl}(\text{NH}_2)_4$ and $\text{NaAl}(\text{NH}_2)_4$, and systematically examined the structural and gas desorption properties by synchrotron X-ray powder diffraction, Fourier-transform infrared spectroscopy, nuclear magnetic resonance spectroscopy, and thermogravimetry coupled with mass spectroscopy.

2. Experimental

To synthesize $M[\text{Al}(\text{NH}_2)_4]_x$, the starting materials, LiH (Alfa Aesar, 99.4%) and Al (Rare metallic, 99.9%) for $M = \text{Li}$ and NaAlH_4 (Aldrich, 90%) for $M = \text{Na}$ and K (Aldrich, 99.95%) and Al for $M = \text{K}$ and Mg (Alfa Aesar, 99.9%) and Al for $M = \text{Mg}$ and CaH_2 (Aldrich, 99.99%) and Al for $M = \text{Ca}$, respectively, were put together into a Cr-steel vessel (SDK-11, UMETOKU Co. Ltd.) with the ratio of $M:\text{Al} = 1:1$ or $1:2$. Then, the vessel was evacuated, bathed into a mixture of dry ice and ethanol, and kept for a while at -79°C . Gaseous NH_3 (5N) was introduced into the vessel and NH_3 was

* Corresponding author at: Institute for Advanced Materials Research, Hiroshima University, Higashi-Hiroshima 739-8530, Japan. Tel.: +81 82 424 5744; fax: +81 82 424 5744.

E-mail address: tichi@hiroshima-u.ac.jp (T. Ichikawa).

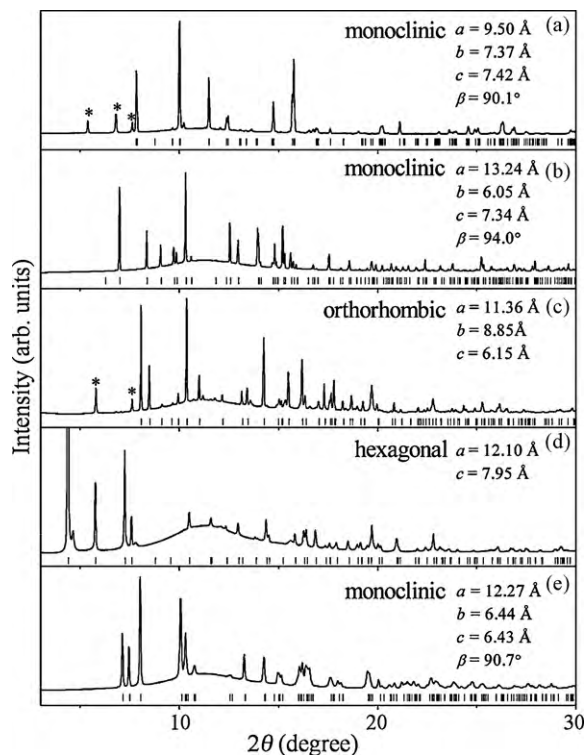


Fig. 1. The SR-XRD patterns of (a) $\text{LiAl}(\text{NH}_2)_4$, (b) $\text{NaAl}(\text{NH}_2)_4$, (c) $\text{KAl}(\text{NH}_2)_4$, (d) $\text{Mg}[\text{Al}(\text{NH}_2)_4]_2$, and (e) $\text{Ca}[\text{Al}(\text{NH}_2)_4]_2$, respectively. Broad features centered at around $2\theta = 11^\circ$ are the background coming from a quartz capillary. Asterisks indicate impurities.

consequently condensed into liquid. Powders were then ball milled in liquid NH_3 for 10, 4, 8, 8, and 10 h for $M = \text{Li}, \text{Na}, \text{K}, \text{Mg},$ and Ca , respectively, at room temperature by a rocking mill apparatus (RM-10, SEIWA GIKEN Co. Ltd.) with a frequency of 10 Hz. In order to avoid the decomposition due to the increase in temperature during the milling treatment, the milling process was interrupted every 15 min for 15 min. To complete the reaction, after the milling process, the milled sample was kept in the vessel for 7 days. Finally, liquid NH_3 was slowly removed at room temperature by a vacuum pump to collect the powder product. All the sample handlings were carried out in a glove box (MP-P60W, Miwa MFG Co. Ltd.) with purified Ar (6N, <1 ppm O_2 and H_2O) to minimize sample degradation.

Structural properties were examined by the synchrotron radiation X-ray diffraction (SR-XRD) measurements at the beamline BL02B2 in SPring-8. The wavelength used was $\lambda = 0.80245(2) \text{ \AA}$ calibrated by the lattice constant of CeO_2 at room temperature. The samples were enclosed in a glass capillary (quartz, $\phi = 0.8 \text{ mm}$) filled with Ar. The Fourier-transform infrared spectroscopy (FT-IR) measurements were performed (Spectrum One, Perkin-Elmer) in a home-made glove box filled with purified Ar. Each sample was diluted by 5 mass% with KBr. ^{27}Al magic-angle spinning (MAS) and triple-quantum MAS (3QMAS) nuclear magnetic resonance (NMR) experiments [11] were performed using a JEOL JNM-ECA600 with the magnetic field of 14.1 T under a spinning rate of 15 kHz. The ^{27}Al chemical shifts were adjusted to an aqueous solution of 1 M AlCl_3 at -0.1 ppm . Sample was filled in a ZrO_2 sample rotor ($\phi = 4 \text{ mm}$) under the Ar atmosphere. Z-filter sequence was used in the 3QMAS experiments [12].

The thermal gas desorption properties were examined by thermogravimetry-differential thermal analysis (TG-DTA; TG8120, Rigaku) installed in the Ar-filled glove box, combined with thermal desorption quadrupole mass spectroscopy (MS; M-QA200TS, Anelva) upon heating to 300°C under He flow. The flow rate was $300 \text{ cm}^3/\text{min}$ and the heating ramp was $5^\circ\text{C}/\text{min}$.

3. Results and discussion

Fig. 1 shows the SR-XRD profiles for $M[\text{Al}(\text{NH}_2)_4]_x$. It is found that they are able to be indexed with single phases with monoclinic ($a = 9.50 \text{ \AA}$, $b = 7.37 \text{ \AA}$, $c = 7.42 \text{ \AA}$, and $\beta = 90.1^\circ$), monoclinic ($a = 13.24 \text{ \AA}$, $b = 6.05 \text{ \AA}$, $c = 7.34 \text{ \AA}$, and $\beta = 94.0^\circ$), orthorhombic ($a = 11.36 \text{ \AA}$, $b = 8.85 \text{ \AA}$, and $c = 6.15 \text{ \AA}$), hexagonal ($a = 12.10 \text{ \AA}$ and $c = 7.95 \text{ \AA}$), and monoclinic ($a = 12.27 \text{ \AA}$, $b = 6.44 \text{ \AA}$, $c = 6.43 \text{ \AA}$, and $\beta = 90.7^\circ$) unit cells for the Li-, Na-, K-, Mg-, and Ca-systems,

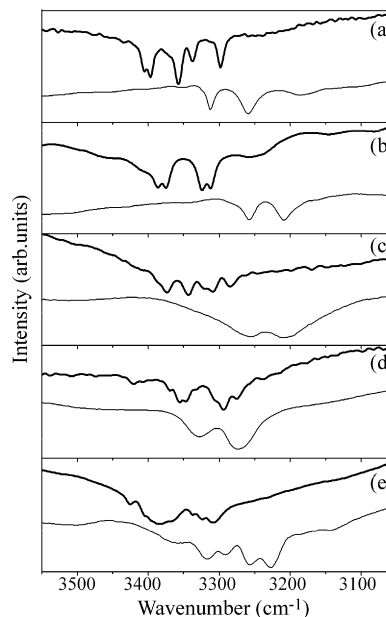


Fig. 2. The FT-IR spectra (N–H vibration) for $M[\text{Al}(\text{NH}_2)_4]_x$ together with the data for $M(\text{NH}_2)_x$ as references; Thick and thin lines correspond to $M[\text{Al}(\text{NH}_2)_4]_x$ and $M(\text{NH}_2)_x$, respectively. (a) $M = \text{Li}$, (b) $M = \text{Na}$, (c) $M = \text{K}$, (d) $M = \text{Mg}$, and (e) $M = \text{Ca}$.

respectively. Our results for $M = \text{Li}$ and Na agree well with the previous reports, indicating that our Li- and Na-samples are actually $\text{LiAl}(\text{NH}_2)_4$ and $\text{NaAl}(\text{NH}_2)_4$, respectively, where an Al atom is coordinated by four $[\text{NH}_2]^-$ units (i.e., anion complex $[\text{Al}(\text{NH}_2)_4]^-$) [6,7,9,13]. On the other hand, the crystal symmetry for our K-sample was different from the previously reported crystal structures for α - and β - $\text{KAl}(\text{NH}_2)_4$ synthesized at -30°C and at room temperature [14–16], suggesting that $\text{KAl}(\text{NH}_2)_4$ has another structure. The crystal structure of $\text{Mg}[\text{Al}(\text{NH}_2)_4]_2$ and $\text{Ca}[\text{Al}(\text{NH}_2)_4]_2$ has never been reported to the best of our knowledge. Also, it should be noted that the Ca-sample is different from calcium aluminum amide ammine complex $\text{Ca}[\text{Al}(\text{NH}_2)_4]_2 \cdot \text{NH}_3$ reported by Palvadeau

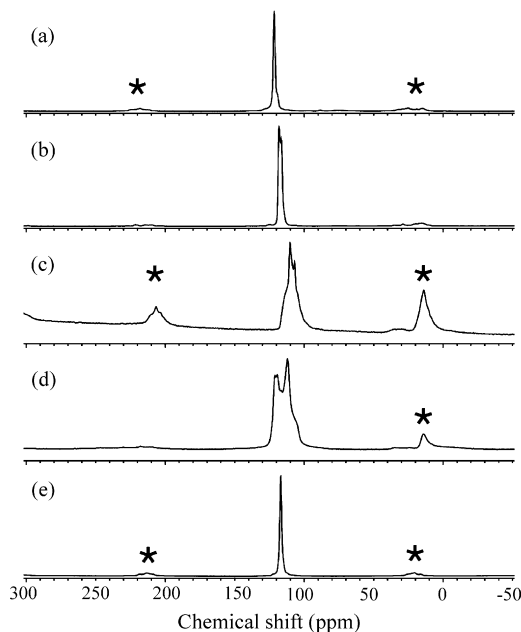


Fig. 3. ^{27}Al MAS NMR spectra of (a) $\text{LiAl}(\text{NH}_2)_4$, (b) $\text{NaAl}(\text{NH}_2)_4$, (c) $\text{KAl}(\text{NH}_2)_4$, (d) $\text{Mg}[\text{Al}(\text{NH}_2)_4]_2$, and (e) $\text{Ca}[\text{Al}(\text{NH}_2)_4]_2$, respectively. Asterisks indicate spinning sidebands.

et al. [17]. The detailed crystal structures for our products will be described elsewhere.

Fig. 2 gives the FT-IR spectra in the frequency region of N–H stretching mode for $M[\text{Al}(\text{NH}_2)_4]_x$ together with those for $M(\text{NH}_2)_x$ as references. The FT-IR spectra of our Li- and Na-samples are very similar to those of $\text{LiAl}(\text{NH}_2)_4$ and $\text{NaAl}(\text{NH}_2)_4$ reported by Jacobs et al. [7] and Lutz et al. [13]. It should be noted that the N–H stretching

vibration ($3250\text{--}3450\text{ cm}^{-1}$) for $\text{LiAl}(\text{NH}_2)_4$ is higher in frequency than that ($3200\text{--}3350\text{ cm}^{-1}$) for LiNH_2 . Similar tendency is also observed for $\text{NaAl}(\text{NH}_2)_4$ and NaNH_2 . The N–H vibrations of the K-, Mg-, and Ca-samples are in a similar frequency region to those of $\text{LiAl}(\text{NH}_2)_4$ and $\text{NaAl}(\text{NH}_2)_4$, strongly suggesting that they all belong to the aluminum amide complex. Again, these metal aluminum amide vibrations are higher in frequency than those for

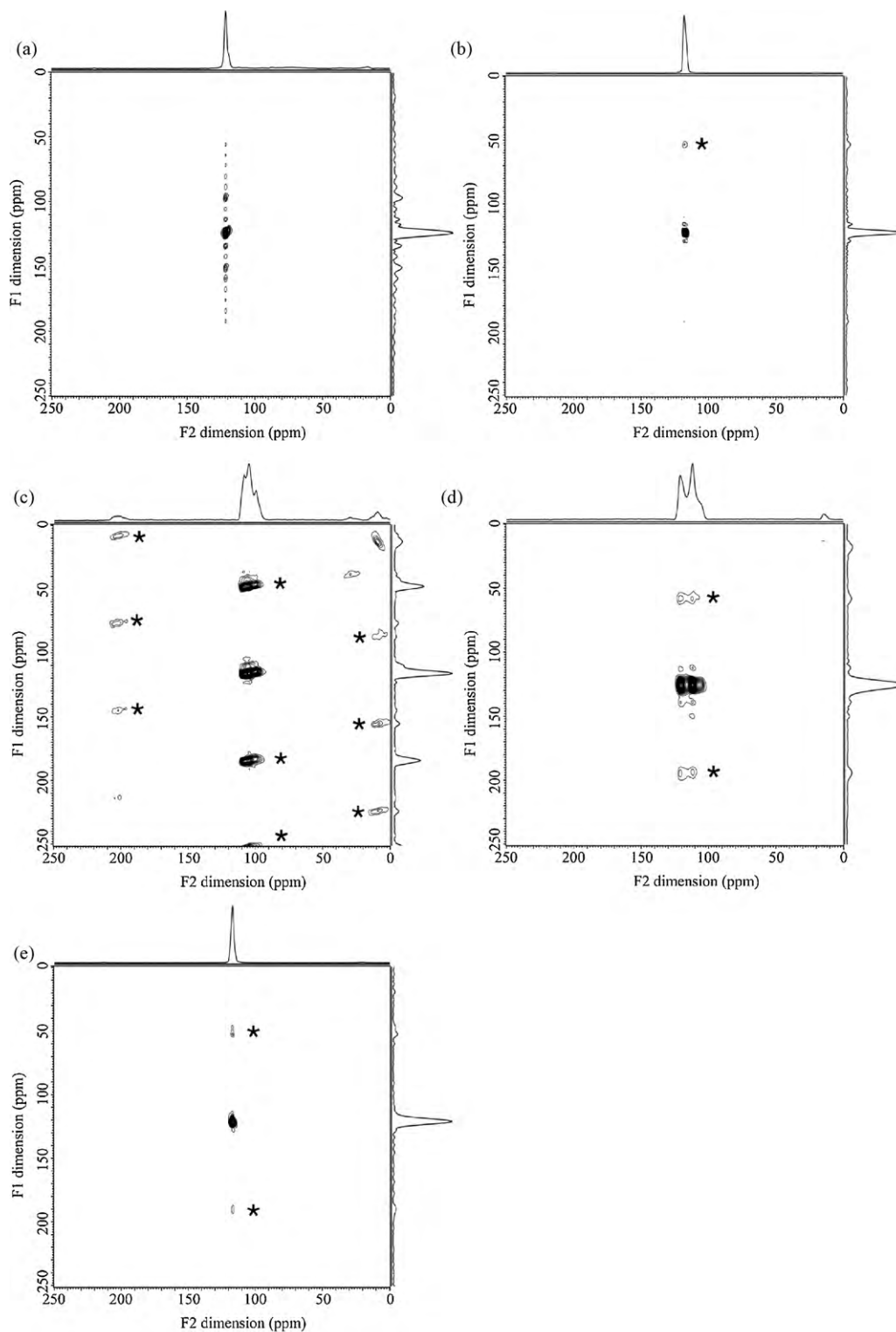


Fig. 4. ^{27}Al 3QMAS NMR spectra of (a) $\text{LiAl}(\text{NH}_2)_4$, (b) $\text{NaAl}(\text{NH}_2)_4$, (c) $\text{KAl}(\text{NH}_2)_4$, (d) $\text{Mg}[\text{Al}(\text{NH}_2)_4]_2$, and (e) $\text{Ca}[\text{Al}(\text{NH}_2)_4]_2$, respectively. Asterisks indicate spinning sidebands. The other small peaks aligned along F1 dimension are due to the artificial ripples coming from the finite FT truncation.

Table 1

The ^{27}Al isotropic chemical shifts δ_{iso} and quadrupolar products P_{q} estimated from the 3QMAS spectra.

Samples	δ_{iso} (ppm)	P_{q} (MHz)
$\text{LiAl}(\text{NH}_2)_4$	123	2.7
$\text{NaAl}(\text{NH}_2)_4$	121	3.4
$\text{KAl}(\text{NH}_2)_4$	116	4.9
$\text{Mg}[\text{Al}(\text{NH}_2)_4]_2$	121	5.4
$\text{Ca}[\text{Al}(\text{NH}_2)_4]_2$	119	3.1

their corresponding metal amides, KNH_2 , $\text{Mg}(\text{NH}_2)_2$, and $\text{Ca}(\text{NH}_2)_2$. This may indicate that Al plays an important role on the N–H bond strength in the aluminum amide complex $[\text{Al}(\text{NH}_2)_4]^-$.

^{27}Al MAS and 3QMAS NMR spectra for our Li-, Na-, K-, Mg-, and Ca-samples are shown in Figs. 3 and 4, respectively. In the MAS spectra, all the products have a peak in the chemical shift range of 100–130 ppm. We observed a single sharp signal for the Li-sample, being consistent with a single Al crystallographic site in $\text{LiAl}(\text{NH}_2)_4$ [6,7]. Taking account of the fact that $\text{NaAl}(\text{NH}_2)_4$ also has a single Al site [9,13], it is found that a small peak splitting observed for the Na-sample is coming from the second-order quadrupolar interaction as is evidenced in Fig. 4(b). The K- and Mg-samples have complex peak shape, but the Ca-sample showed a single sharp peak. The isotropic projections (lateral spectra in Fig. 4) of the ^{27}Al 3QMAS spectra of the K- and Mg-samples unambiguously indicate that they also have a single Al site. The ^{27}Al isotropic chemical shifts δ_{iso} and quadrupolar products P_{q} estimated from the 3QMAS spectra are listed in Table 1. The obtained δ_{iso} of 116–123 ppm indicates tetrahedral Al sites in our products. Also, the large P_{q} values of K- and Mg-samples imply significant distortions on the tetrahedral Al sites. Combined with the SR-XRD and FT-IR results, therefore, we conclude that we successfully synthesized metal aluminum amides $\text{KAl}(\text{NH}_2)_4$, $\text{Mg}[\text{Al}(\text{NH}_2)_4]_2$, and $\text{Ca}[\text{Al}(\text{NH}_2)_4]_2$, along with the already reported $\text{LiAl}(\text{NH}_2)_4$ and $\text{NaAl}(\text{NH}_2)_4$, where an Al atom is covalently coordinated by four amide units $[\text{NH}_2]^-$ and cations M^+ or M^{2+} play a charge-balancing role.

Fig. 5 shows the TG-DTA curves and the NH_3 desorption profiles (mass number = 17) for the $M[\text{Al}(\text{NH}_2)_4]_x$ samples. The H_2 gas desorption was not observed above the detection limit. The sample weights suddenly started to decrease with releasing NH_3 gas at low temperatures of 100, 85, 49, 116, and 82 °C and the NH_3 desorption peak temperatures T_{des} in the MS profiles were 136, 92, 58, 132, and 107 °C for $M = \text{Li}, \text{Na}, \text{K}, \text{Mg},$ and Ca , respectively. DTA curves showed that $M[\text{Al}(\text{NH}_2)_4]_x$ released NH_3 by endothermic reaction at T_{des} . It is noteworthy that T_{des} of $M[\text{Al}(\text{NH}_2)_4]_x$ are much lower than those of $M(\text{NH}_2)_x$ [4,18–20]. The released NH_3 molecules estimated from the weight losses are listed in Table 2. This indicates that a considerable amount of NH_3 is able to be released above the peak temperatures. Also, the gradient of the TG curve changed drastically above the peak temperature. These results indicate that

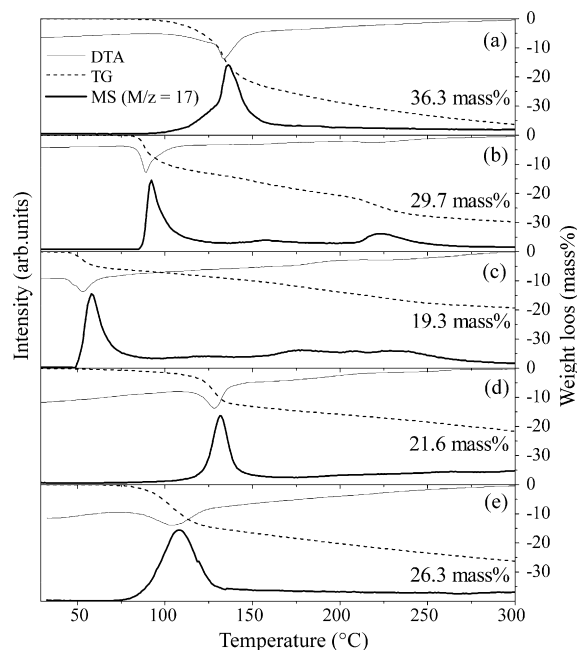


Fig. 5. The TG-DTA-MS profiles for (a) $\text{LiAl}(\text{NH}_2)_4$, (b) $\text{NaAl}(\text{NH}_2)_4$, (c) $\text{KAl}(\text{NH}_2)_4$, (d) $\text{Mg}[\text{Al}(\text{NH}_2)_4]_2$, and (e) $\text{Ca}[\text{Al}(\text{NH}_2)_4]_2$. Thick and thin solid lines correspond to the NH_3 desorption profile (M/z , mass number = 17) and DTA curves, respectively. Dashed line indicates the weight loss (the values at 300 °C are shown).

Table 2

The released NH_3 molecules at the end of peak temperatures.

Samples	Released NH_3 (molecule per $M[\text{Al}(\text{NH}_2)_4]_x$)	
	T_{e}	300 °C
$\text{LiAl}(\text{NH}_2)_4$	1.4 (160 °C)	2.1
$\text{NaAl}(\text{NH}_2)_4$	0.8 (108 °C)	2.0
$\text{KAl}(\text{NH}_2)_4$	0.5 (72 °C)	1.5
$\text{Mg}[\text{Al}(\text{NH}_2)_4]_2$	1.5 (144 °C)	2.6
$\text{Ca}[\text{Al}(\text{NH}_2)_4]_2$	1.9 (129 °C)	3.4

the NH_3 desorption in $M[\text{Al}(\text{NH}_2)_4]_x$ proceeds in at least two-step processes.

We found that T_{des} decreased with their increasing atomic number on the respective alkali and alkaline-earth aluminum amides, i.e., $T_{\text{des}}(\text{Li}) > T_{\text{des}}(\text{Na}) > T_{\text{des}}(\text{K})$ and $T_{\text{des}}(\text{Mg}) > T_{\text{des}}(\text{Ca})$. This suggests that the kind of cation M has an influence on the NH_3 desorption temperature, in other words, on the thermal stability of $M[\text{Al}(\text{NH}_2)_4]_x$. Here, there appears to be a positive correlation between T_{des} , and ^{27}Al isotropic chemical shift and the Pauling's electronegativity χ_{p} [21] of a cation M as shown in Fig. 6. When $M = \text{Li}$ is replaced by Na and K, χ_{p} decreases from 0.98 (for Li) to

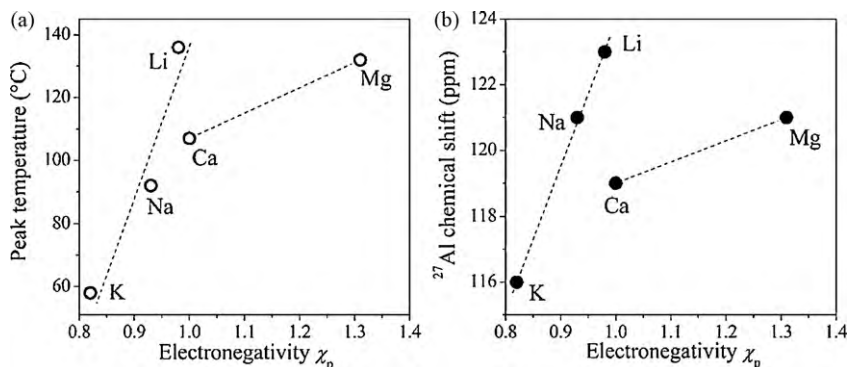


Fig. 6. Relationships (a) between electronegativity of cation M and peak temperature of NH_3 desorption, and (b) between electronegativity and ^{27}Al isotropic chemical shift.

0.93 (for Na) and 0.82 (for K), T_{des} decreases from 136 °C to 92 and 58 °C, respectively. ^{27}Al isotropic chemical shift similarly decreases from 123 ppm to 121 and 116 ppm. This tendency is also observed for the alkali-earth system, $M = \text{Mg}$ and Ca . It is interesting to note that the $T_{\text{des}} - \chi_{\text{p}}$ relationship for $M[\text{Al}(\text{NH}_2)_4]_x$ shows an opposite tendency to that for metal borohydrides $M[\text{BH}_4]_n$ ($M = \text{Mg}$, Ca – Mn , Zn , Al , Y , Zr and Hf ; $n = 2$ – 4), where T_{des} decreases as a function of χ_{p} of M [22]. We here try to rationalize the relationship between T_{des} and magnetic shielding on the Al site. When the atomic number of the cation is increased (*i.e.*, χ_{p} decreases), the difference of χ_{p} between the cation and nitrogen in $[\text{Al}(\text{NH}_2)_4]^-$ becomes larger. Increasing the electron from the cation to nitrogen will reduce the electron donated from Al to nitrogen. That causes Al having higher charge density, which increases magnetic shielding effect on the Al nucleus and gives a negative frequency shift (Table 1). Reducing the electron donation from Al to nitrogen suggests weakening the Al–N bonds to lower the NH_3 desorption temperature. This indicates that the thermal stability of $M[\text{Al}(\text{NH}_2)_4]_x$ can be driven by the choice of the cation M . In addition, the $T_{\text{des}} - \chi_{\text{p}}$ relationship for $M[\text{Al}(\text{NH}_2)_4]_x$ shows different tendencies in the groups of IA and IIA, which should be quite different from the tendency reported on $M[\text{BH}_4]_n$ by Nakamori et al. [22].

4. Conclusions

Metal aluminum amides $M[\text{Al}(\text{NH}_2)_4]_x$ ($M = \text{Li}$, Na , K , Mg , and Ca ; $x = 1$ and 2) were successfully prepared by mechanical milling under liquid NH_3 condition. Structural characterization was performed by SR-XRD, FT-IR, and solid state NMR techniques. The crystal structures of $\text{LiAl}(\text{NH}_2)_4$ and $\text{NaAl}(\text{NH}_2)_4$ were identical to those previously reported. On the other hand, $\text{KAl}(\text{NH}_2)_4$, $\text{Mg}[\text{Al}(\text{NH}_2)_4]_2$, and $\text{Ca}[\text{Al}(\text{NH}_2)_4]_2$ were found to be novel metal aluminum amides. They all have an anion complex $[\text{Al}(\text{NH}_2)_4]^-$, where $[\text{NH}_2]^-$ is covalently bonded with Al, and cations M^+ or M^{2+} are charge balancing. TG-DTA-MS profiles showed that $M[\text{Al}(\text{NH}_2)_4]_x$ started to release the NH_3 gas at around 100 °C, much lower temperatures than that shown by $M(\text{NH}_2)_x$. We found that the NH_3 desorption temperature decreased with the increasing atomic number of respective alkali and alkaline-earth cations in $M[\text{Al}(\text{NH}_2)_4]_x$. We further observed that ^{27}Al isotropic chemical shift was correlated with the desorp-

tion temperature, which may suggest that the weakening of Al–N bonds involves the NH_3 gas release. This means that the NH_3 desorption temperature can be controlled by replacing the cation, and thus could provide a new insight for hydrogen storage application when the $\text{MH}-M'[\text{Al}(\text{NH}_2)_4]_x$ composite materials are prepared.

Acknowledgement

This work was partially supported by the NEDO project “Advanced Fundamental Research Project on Hydrogen Storage Materials”. The SR-XRD experiments were performed at the SPRING-8 with the approval of the Japan Synchrotron Radiation Research Institute (JASRI) (Proposal No. 2008B2101).

References

- [1] L. Schlapbach, A. Züttel, *Nature* 414 (2001) 353–358.
- [2] P. Chen, Z. Xiong, J. Luo, J. Lin, K.L. Tan, *Nature* 420 (2002) 302–304.
- [3] S.J. Pawel, *J. Nucl. Mater.* 218 (1995) 302–313.
- [4] T. Ichikawa, N. Hanada, S. Isobe, H. Leng, H. Fujii, *J. Phys. Chem. B* 108 (2004) 7887–7892.
- [5] R. Janot, J. Eymery, J. Tarascon, *J. Phys. Chem. C* 111 (2007) 2335–2340.
- [6] J. Rouxel, R. Brec, *C. R. Acad. Sci. Paris C* 262 (1966) 1071–1073.
- [7] H. Jacobs, K. Ja'nichen, C. Handenfeidt, R. Juza, *Z. Anorg. Allg. Chem.* 531 (1985) 125–139.
- [8] N. Aliouane, T. Ono, O.M. Lovvik, M. Tsubota, T. Ichikawa, Y. Kojima, B.C. Hauback, submitted for publication.
- [9] R. Brec, J. Rouxel, *C. R. Acad. Sci. Paris C* 264 (1967) 512–515.
- [10] H. Jacobs, B. Nöcker, *Z. Anorg. Allg. Chem.* 619 (1993) 381–386.
- [11] L. Frydman, J.S. Harwood, *J. Am. Chem. Soc.* 117 (1995) 5367–5368.
- [12] J.-P. Amoureux, C. Fernandez, S. Steuernagel, *J. Magn. Reson. A* 123 (1996) 116–118.
- [13] H.D. Lutz, N. Lange, H. Jacobs, B. Nöcker, *Z. Anorg. Allg. Chem.* 613 (1992) 83–87.
- [14] P.P. Molinie, R. Brec, J. Rouxel, P. Herpin, *Acta Cryst. B* 29 (1973) 925–932.
- [15] R. Brec, P. Palvadeau, P. Herpin, *C. R. Acad. Sci. Paris C* 274 (1972) 266–268.
- [16] R. Brec, J. Rouxel, *Bull. Soc. Chim. Fr.* 7 (1968) 2721–2726.
- [17] P. Palvadeau, M. Drew, G. Charlesworth, J. Rouxel, *C. R. Acad. Sci. Paris C* 275 (1972) 881–884.
- [18] A.W. Titherley, *J. Chem. Soc. Trans.* 65 (1894) 504–522.
- [19] H.Y. Leng, T. Ichikawa, S. Hino, N. Hanada, S. Isobe, H. Fujii, *J. Phys. Chem. B* 108 (2004) 8763–8765.
- [20] S. Hino, T. Ichikawa, H. Leng, H. Fujii, *J. Alloys Compd.* 398 (2005) 62–66.
- [21] D.R. Lide (Ed.), *CRC Handbook of Chemistry and Physics*, 89th ed., CRC Press, 2008.
- [22] Y. Nakamori, H.-W. Li, M. Matsuo, K. Miwa, S. Towata, S. Orimo, *J. Phys. Chem. Solids* 69 (2008) 2292–2296.